The Effect of Unheated Sections on Moisture Transport in the Emplacement Drift

G. Danko and D. Bahrami
Mackay School of Mines
University of Nevada, Reno
Reno, NV 89557
(775) 784-4284
danko@unr.edu, davood@scs.unr.edu

J.T. Birkholzer
LBNL, Earth Science Division, MS 90-116
1 Cyoloton Rd.
Berkeley, CA 94720
(510)486-7134
JTBirkholzer@lbl.gov

Abstract - *A thermal-hydrologic –natural-ventilation model is configured for simulating temperature, humidity, and condensate distributions in the coupled domains of the in-drift airspace and the near-field rockmass. Meaningful results are obtained from the model for a practical application in which the beneficial effects of unheated drift sections are analyzed. Sensitivity to the axial dispersion coefficient is also studied with the model.*

I. INTRODUCTION

A research project is underway with the purpose of improving understanding of the coupling between thermo-hydrological processes (including air and vapor movement) in the in-drift, near-field, and mountain-scale systems at Yucca Mountain (YM). Specific aims are (1) to a configure, test, and verify a novel, efficient, numerical-computational, coupled model; and (2) to evaluate the coupled, in-drift heat and moisture transport with evaporation, condensation, and seepage of water into drifts from the near-field rockmass at different stages after waste emplacement. These objectives are met by developing a multi-scale modeling approach that (1) integrates in-drift and in-rock process models in a consistent, transparent, and scientifically defensible manner; and (2) allows for studying the storage environment in various emplacement drifts without applying excessive conservatism in the modeling assumptions. The paper describes some early results of the model, specifically a study on the effects of unheated drift end sections.

II. A MULTI-SCALE, COUPLED NUMERICAL-COMPUTATIONAL MODEL

II.A. Model Concept

A specific aim of the model formulation is to describe the physical processes that contribute to the formation of a robust natural barrier for water reaching waste packages for several thousands of years. The rockmass domain around an emplacement drift is treated as a coupled, mountain-scale connection between hot and cold drift sections. The in-drift moisture transport along the drift length as well as the condensate trapping process is modeled in order to be harnessed for moving water away from the waste packages. Instead of trying to mitigate the negative effects of humidity variations and condensate trapping, the transport processes are used to verify new technology concepts.

A numerical-computational modeling method is used that integrates known solution elements. The problem to be solved is the coupled, near-field and in-drift thermal, hydrologic, natural air movement, and condensation processes with mountain-scale effects at YM. The coupled, in-rock and in-drift transport processes are modeled using MULTIFLUX [1] (MF) with (1) TOUGH2 [2] for the in-rock processes both above and below the drift in the unsaturated zone (UZ); (2) a lumped-parameter Computational Fluid Dynamic (CFD) model for the in-drift transport processes, including natural air convection and condensation around the waste packages (WPs); and (3) an iterative coupler for enforcing boundary coupling of the heat and moisture transport processes on the interface between the drift air space and the rockmass surrounding the drift. MF applies an innovative, surrogate model-element, obtained from a Numerical Transport Code Functionalization (NTCF) procedure [3], reducing the number of TOUGH2 runs during iteration. Support data for in-drift airflow and dispersion coefficients are currently imported from a CFD simulation from the literature [4,5] based on calculations with the commercial CFD code FLUENT.

II.B. Thermal-hydrologic Model of the Rockmass

A multi-scale rockmass model is prepared to identify a representative NTCF model using the TOUGH2 thermal-hydrologic porous-media code. Figure 1 shows the rockmass domain with an emplaced drift as a three-dimensional (3-D) slice of the mountain in the middle of an emplacement panel. Sufficiently large unheated areas at both ends of the emplacement drift are included in the model domain. Rock properties and boundary conditions on the surface and at the watertable are essentially identical to those of previous studies [6,7].

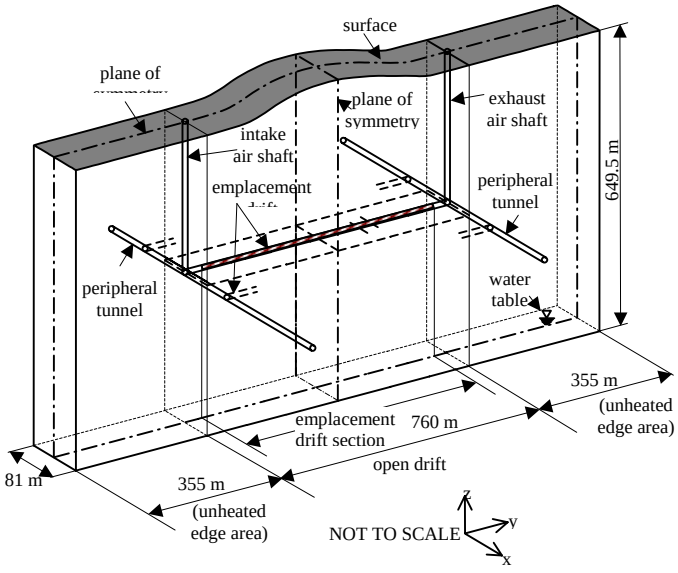

Figure 1: Rockmass Domain around an Emplacement Drift in Panel 2

A pre-selected set of drift surface temperature, *T*, and partial vapor pressure, *P*, variations are used as additional boundary conditions in the TOUGH2 model to generate heat flux, *qh*, and moisture flux, *qm*, responses on the rock-air interface along the entire drift length and over a post-closure time period of 5000 years. Along the length of the drift, 44 individual mountain-scale divisions are applied. The relationship between the set of input *T*, *P,* and output *qh, qm* temporal variations for each drift section define the corresponding mountain-scale rockmass NTCF model for heat and moisture. The following matrix equation terms are selected for the NTCF model:

$$qh = qh^c + hh \cdot \left(T - T^c\right) + \left\langle T \right\rangle \cdot hm \cdot \left(P - P^c\right) \quad (1)$$

$$qm = qm^c + mh \cdot \left(T - T^c\right) + \left\langle T \right\rangle \cdot mm \cdot \left(P - P^c\right) \quad (2)$$

The *hh*, *hm*, *mh*, and *mm* dynamic admittance matrices are identified based on Eqs (1) and (2) by fitting *qh* and *qm* to TOUGH2 data. The NTCF model identification method follows the technique described in [3]. The model for each drift-section perfectly reproduces qh^c and qm^c, the central output fluxes from TOUGH2, for $T=T^c$ and $P=P^c$, the central input boundary conditions, that are included in the pre-selected set of boundary conditions.

Other *T* and *P* input variations can produce outputs from the NTCF model for *qh* and *qm* without actually re-running TOUGH2. Figure 2 shows comparison between the TOUGH2 and NTCF heat and moisture flux results for 22 models (i.e., for each of the 22 divisions along a half drift length) over a 5000 year time period. In Fig 2, the input *T* and *P* variations are +5% deviated from the T^c and P^c central values for which *qh* and *qm* vectors are calculated from Eqs (1) and (2). For the coupled in-rock and in-drift model, 454 drift-scale NTCF models are generated from the mountain-scale NTCF models by scaling, following the technique used in [8].

II.C. CFD Models for Heat and Moisture Transport in the Emplacement Drift

The lumped-parameter, in-drift CFD model configuration includes 80 m long, unheated sections with heat and mass transport connections to the hot drift sections along them. A uniform heat load is assumed for each waste package in the drift, although this stipulation is not a necessity for the solvability of the model. Other data inputs for the CFD model for heat and moisture transport essentially agree with those of a previous study [6].

The energy balance equation in the CFD model of MF is used in a simplified form, as follows, for an *x*-directional flow with v_i velocity in a flow channel of cross section *dy* by *dz*:

$$\rho c \frac{\partial T}{\partial t} + \rho c v_i \frac{\partial T}{\partial x} = \rho c a \frac{\partial^2 T}{\partial x^2} + \rho c a \frac{\partial^2 T}{\partial y^2} + \rho c a \frac{\partial^2 T}{\partial z^2} + \dot{q}_h \quad (3)$$

In Eq. (3), ρ and *c* are density and specific heat of moist air, respectively, *a* is the molecular or eddy thermal diffusivity for laminar or turbulent flow, and $\dot{q}_h$ is the latent heat source or sink for condensation or evaporation. In turbulent shear and boundary layer flows, *a* is different in *x*, *y*, and *z*. directions and may be substituted with direction-specific values for the effective dispersion coefficients. The second and the third terms on the right-hand-side of Eq. (3) represent heat conduction (or effective heat conduction) in the normal, *x* and *y* directions to the x axis of the flow channel; these terms are substituted with expressions for transport connections using heat transport coefficients for flow channels bounded by solid walls. Eq. (3) is discretized and solved numerically and simultaneously along all flow channels for the temperature field *T* in MF. The flow channels represent the natural coordinate system of the flow field that must be known for the calculations.

The simplified moisture transport convection-diffusion equation in the CFD model of MF is similar to Eq. (3) as follows:

$$\frac{\partial \rho_v}{\partial t} + v_i \frac{\partial \rho_v}{\partial x} = D \frac{\partial^2 \rho_v}{\partial x^2} + D \frac{\partial^2 \rho_v}{\partial y^2} + D \frac{\partial^2 \rho_v}{\partial z^2} + \dot{q}_{cm} + \dot{q}_{sm} \quad (4)$$

In Eq. (4), ρ_v is the partial density of water vapor, *D* is the molecular or eddy diffusivity for vapor (equated with the effective moisture dispersion coefficient in

turbulent flow), $\dot{q}_{cm}$ is the moisture source or sink due to condensation or evaporation, and $\dot{q}_{sm}$ is the vapor flux in superheated steam form.

It is possible to reduce the number of discretization elements in the computational domain by lumping nodes. MF allows for defining connections between lumped volumes, applying direct heat and moisture transport relations between them. The current lumped-parameter CFD model in the drift applies 15x454 nodes for the heat, and the same number of nodes for the moisture transport. Each WP is represented by two nodes, with one additional node for the gap between neighboring containers. CFD nodes are in the airway along three longitudinal lines: close to the drip shields, close to the drift wall above the drip shields, and close to the side wall, with 454 nodes on each line. The drift inside wall is assumed to be separated from the rock wall with a 10^{-5} m-thick still air layer, and are both represented by 454 nodes each along three lines: at the invert, sidewall, and roof. The sidewall and the crown of the drip shields are represented by two lines with 454 nodes on each. The airspace under the drip shields are modeled also by three lines each having 454 nodes. In addition, 3x454 nodes represent the rock-air interface, making the total number of nodes in the CFD model for heat 8172. The same number of nodes is used in the CFD model for moisture transport.

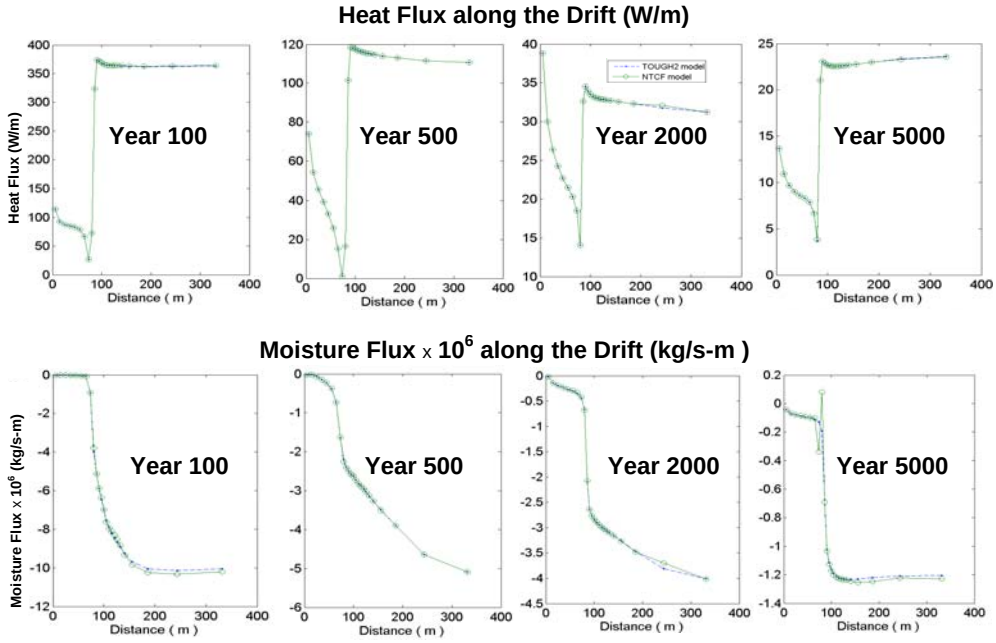

Figure 2. Comparison between the heat and moisture flux results from TOUGH2 and the NTCF model. The 22 points along a half-drift length in the heat and moisture flux curves are from 22 individual NTCF models. Note that the first 80 m of drift section has no WPs.

Figure 3 is a simplified illustration of both heat and moisture transport connections. Heat and moisture transport are modeled using heat and moisture transport coefficients at the WP, drift wall, and at both sides of the drip shields. 3-D thermal radiation between solid surfaces is also included in the CFD models.

Natural, secondary flow is considered due to the local temperature differences in the drift. The mean axial airflow is assumed to be zero in the present case, unlike in a previous study [8] in which a slow, axial in-drift airflow was assumed. In each drift segment of a half-WP length, the re-circulating mass flow rate in vertical direction is taken as 0.04 kg/s, a constant value for the study time period between 60 and 5,000 years, based on the FLUENT simulation results of natural convection studied by Webb and Itamura [4,5]. The mass flow rate in vertical direction is used to calculate velocities along the air recalculation transport loops during the lumped-parameter CFD solution. The axial connection between the air nodes are bi-directional, modeled with constant dispersion coefficients, published for a similar emplacement drift with axial thermal gradient ("with temperature tilt") and without axial thermal gradient ("without temperature tilt") [4,5]. The dominantly natural heat transport coefficient on the drift, waste package, and drip shield walls during post-closure are all set to a constant value of 1.85 W/(m^{2}K), a value consistent with the results of more detailed numerical modeling [4].

II.D. Coupled In-rock NTCF and In-drift CFD Models

The NTCF and CFD models are coupled on the rock-air interface by MF until the heat and moisture flows are balanced at the common surface temperature and

partial vapor pressure at each surface node and time instant. Two iteration loops are used in the current study:

1. Heat flow balance iteration between the NTCF and airway CFD models for each time division.
2. Moisture flow balance iteration between the NTCF and airway CFD models for each time division.

The simulation results obtained from the CFD model elements are temperature, relative humidity, and water condensate variations within the emplacement drift, including distributions on the drift wall boundary. The main focus of a study may be directed to the processes in the rockmass and not in the drift, such as in [9]. Temperature, humidity, and moisture flow distributions in the rockmass, already coupled to the in-drift processes, are given by the TOUGH2 porous-media model. Read-out of saturation and/or moisture flow results at any time instant must be made during the MF runs at the end of a successful iteration for heat and moisture flow balances.

III. COUPLED SIMULATION RESULTS

The power of the modeling method is demonstrated using four different CFD model configurations while keeping the NTCF rockmass model unchanged.

III.A. High Axial Dispersion Case, Sealed and Un-sealed Unheated Drift Sections

First, an axial dispersion coefficient of 0.1 m^2/s was used from literature [4,5]. Temperature, humidity, and water condensate results were obtained from the balanced, fully coupled, multi-scale model for the baseline arrangement with 80 m unheated, un-sealed drift sections, shown in Fig 4.a.

Spatial and temporal, temperature and relative humidity distributions are given in 3-D plots in Figures 5a and b for the unsealed drift in which the unheated sections are in a common airspace with the active middle section. Thick lines in Figure 5a and b mark the position of the first and the last WP in the drift. As shown, the relative humidity along the active emplacement area between the two thick lines is well below 100% saturation over the entire 5000 years.

The study was repeated for a modified drift arrangement in which the moisture transport was blocked by impermeable seals at the first and last waste packages shown in Fig 4.b. The effect of the blockages is simulated in the CFD model by eliminating the axial moisture transport connections between the heated and unheated drift sections at two given locations. These blockages are assumed to cut moisture transport from the hot, emplaced drift section to the cold, empty drift sections. The thermal connections were not changed in the model. Figure 6a and b are temperature and relative humidity distributions in 3-D format for the drift arrangement with sealed-off unheated sections. As shown, the relative humidity along the drift length is not monotonous: saturation peaks to 100% first within the active emplacement section, and peaks again in the unheated section.

Temperature, relative humidity, and condensate distributions along the drift length at six time instants are shown in Figure 7a, b and c for both un-sealed (solid lines) and sealed-off unheated drift sections (dashed lines). As shown, the long, unheated drift sections significantly reduce the relative humidity in the emplacement drift along the WPs. No condensation is found on the wall, drip shield, or WPs within the study time period in the active emplacement drift section. In comparison, the arrangement with no unheated drift sections shows significantly higher relative humidity distribution along the active drift section. However, only the locations of the two coldest waste packages develop condensation, acting as drainage sinks in the emplacement drift.

III.B. Low Axial Dispersion Case, Sealed and Un-sealed Unheated Drift Sections

Second, a low axial dispersion coefficient of 0.004 m^2/s was assumed, following also [4,5]. The study with the low dispersion coefficient also included two model runs, one with the unsealed, unheated sections to establish baseline results, and one with the seals in the moisture transport model. The results of the low axial dispersion coefficient study are shown in Figure 8a, b and c for temperature, relative humidity, and condensate at six selected time instants. Results for the baseline and the sealed-off arrangements are shown respectively, in solid and in dashed lines in Figures 8a, b and c. As depicted, the benefit of long, unsealed, unheated drift section in the emplacement drift is not as strong in the low axial dispersion case as in the one with high axial dispersion coefficient. If the axial transport is not strong enough for carrying away the vapor and superheated steam from the hot drift section to the cold ends, the relative humidity is not reduced considerably in the middle drift section by the axial moisture transport. Condensation is predicted at some cold spots such as at the gaps between waste packages. However, some benefits are still seen in humidity and seepage/condensate reduction.

III.C. Discussion of the Dispersion Coefficient Model

The high sensitivity of vapor transport results to the value of the axial dispersion coefficient warrants close attention. Within the drift airspace, stagnant, as well as highly turbulent airflow domains are present, depending on the natural buoyancy driving forces caused by temperature

differences in a particular location. Molecular diffusion coefficient for air in an air-vapor mixture is D_0 = 2.13 x 10^{-5} m^2/s [2], while the overall, average, axial dispersion coefficient in a turbulent, mixing flow may be as high as 0.1 m^2/s [4,5]. These values, over-arching three orders of magnitude, co-exist in an emplacement drift. It will be highly desirable to apply location- and temperature-specific dispersion coefficient values in the lumped-parameter CFD model in the future.

A possible solution is to determine a numerical-empirical relationship between the axial dispersion coefficient and the axial temperature difference for the axial convection cells, in non-dimensional form based on existing data [4,5] and/or new FLUENT simulations. The lumped-parameter CFD model in MF then can be used to incorporate location- and temperature-dependent values in the coupled model solution. An example of such a non-dimensional expression for the dispersion coefficient may be obtained from a fitting exercise as follows:

$$D = D_0\left\{1+76Ra_{L_C,\Delta T_r}^{0.05}\left[1+0.05\left(\frac{L_C}{L}\right)Ra_{L_C,\Delta T_L}^{0.5}\right]\right\} \quad (5)$$

In Eq (5), $Ra_{Lc,\Delta Tr}$, following [4,5], is the Rayleigh number calculated with the gap-width characteristic length, L_C, and temperature difference in radial direction; and $Ra_{Lc,\Delta TL}$, is the Rayleigh number calculated with the same characteristic length but with a temperature difference over the axially connected distance, L, along the drift length. Eq (5) fits quite well to existing data [4,5] shown in Table 1. The model may reduce CFD input uncertainty from three orders of magnitude to a few tens of percent.

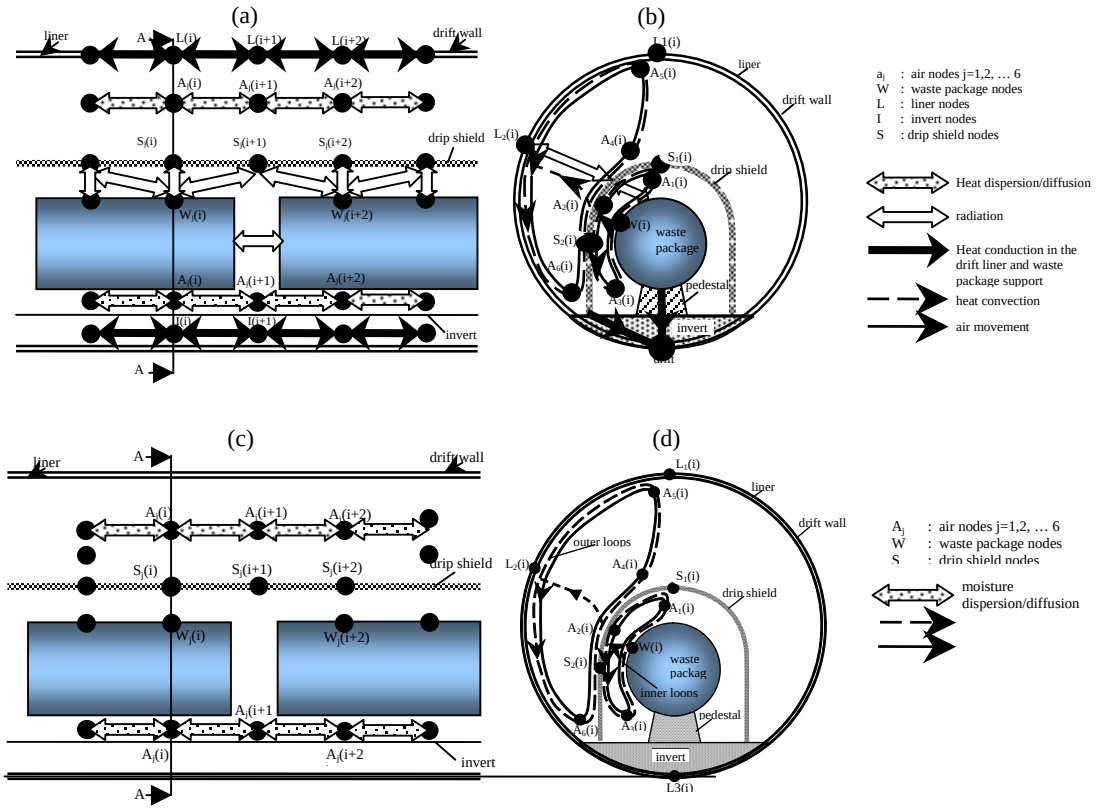

Figure 3. In-drift lumped parameter CFD; for heat in axial direction (a); for heat in A-A cross section (depicted only on the left-hand-side of the symmetrical figure) (b); for moisture in axial direction (c); and for moisture in A-A cross section (d) (depicted only on the left-hand-side of the symmetrical figure).

Table 1. Comparison of dispersion coefficient values (m^2/s) between Equation (5) and published results [4,5]

		Without Temperature Tilt		With Temperature Tilt	
		1000 Yrs	**3000 Yrs**	**1000 Yrs**	**3000 Yrs**
Under Drip Shield	**From [4,5]**	0.006	0.007	0.007	0.009
	From Eq(5)	0.004	0.004	0.009	0.008
Outside Drip Shield	**From [4,5]**	0.004	0.004	0.1	0.1
	From Eq(5)	0.004	0.004	0.1	0.081

CONCLUSIONS

A fully-coupled, in-drift and near-field, in-rock model is configured and applied for the solution of a complex thermo-hydrologic-airflow problem at YM.

As a coupled thermal-hydrologic model exercise, the beneficial effect of elongated, unheated emplacement drift sections at both ends was studied and comparatively evaluated. No condensation was found around the WPs, and an improvement to the results for a drift arrangement without the long unheated sections was achieved in the high axial dispersion coefficient case.

Lower condensation rates and fewer condensation locations in the emplacement drift are predicted with the present model than those obtained using an approximate, and basically un-coupled condensation model [5].

The application of an unheated drift section for decreasing humidity in the emplacement drift has been studied before [10], although in a different arrangement in which a slow air re-circulation along the drift was engineered. The current result once again illustrates the benefit of maintaining unheated, low-temperature sections in the drift airspace in order to lower the relative humidity in the active emplacement drift section. Significant sensitivity to the axial dispersion coefficient in the emplacement drift is found. This fact underlines the importance of a fast-running, efficient modeling method, since input data variations will likely be needed in future studies and design exercises.

The range of the values for axial dispersion coefficient arches over three orders of magnitude from molecular diffusion to turbulent dispersion in an emplacement drift. In order to reduce uncertainties, it will be important to use location-specific, temperature field dependent coefficients in the lumped-parameter CFD model instead of overall constants for the entire drift in future studies. Such a dispersion coefficient model example is given in Eq (5), derived as a fitting exercise.

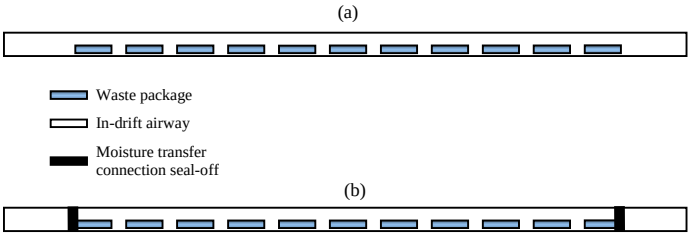

Figure 4. Sectional view of the emplacement drift for the case of unheated sections not sealed (a); and unheated section sealed off (b).

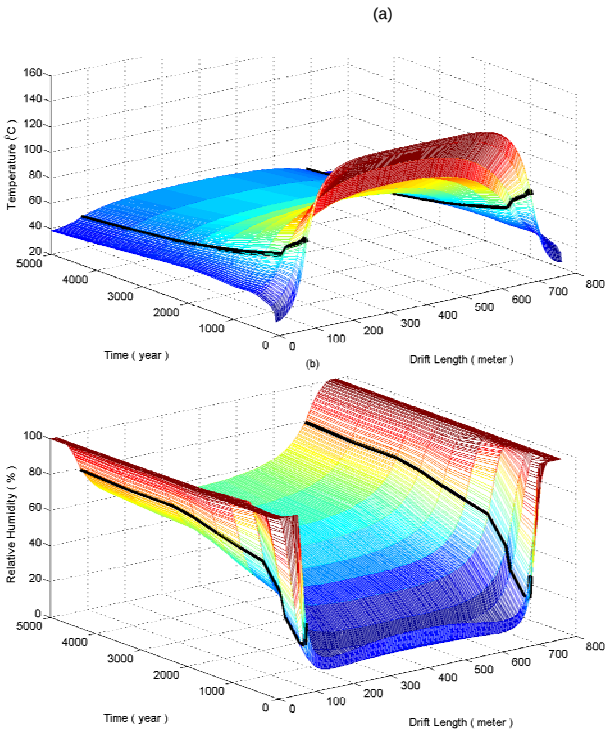

Figure 5. Drift Wall Temperature (a); and Relative Humidity Distributions (b) for case of unheated sections not sealed. The a axial moisture dispersion coefficient is 0.1 m^2/s.

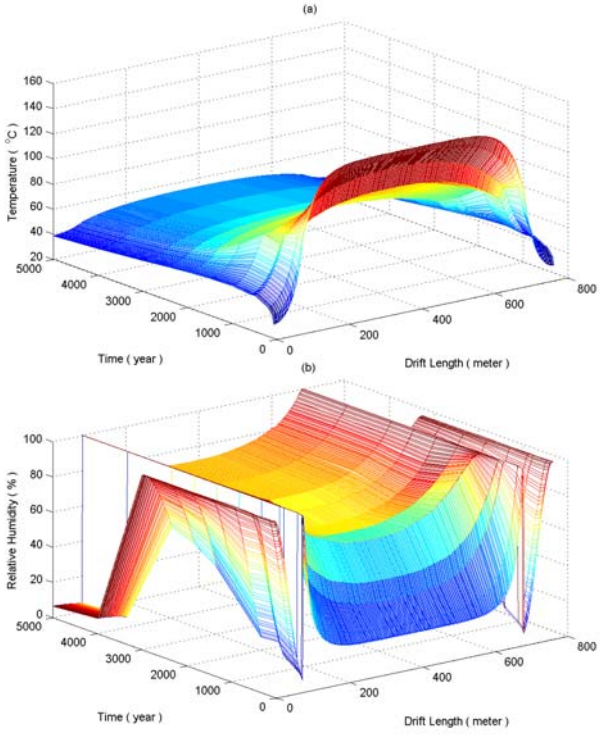

Figure 6. Drift Wall Temperature (a); and Relative Humidity Distributions (b) for case of unheated sections sealed off. The axial moisture dispersion coefficient is 0.1 m^2/s.

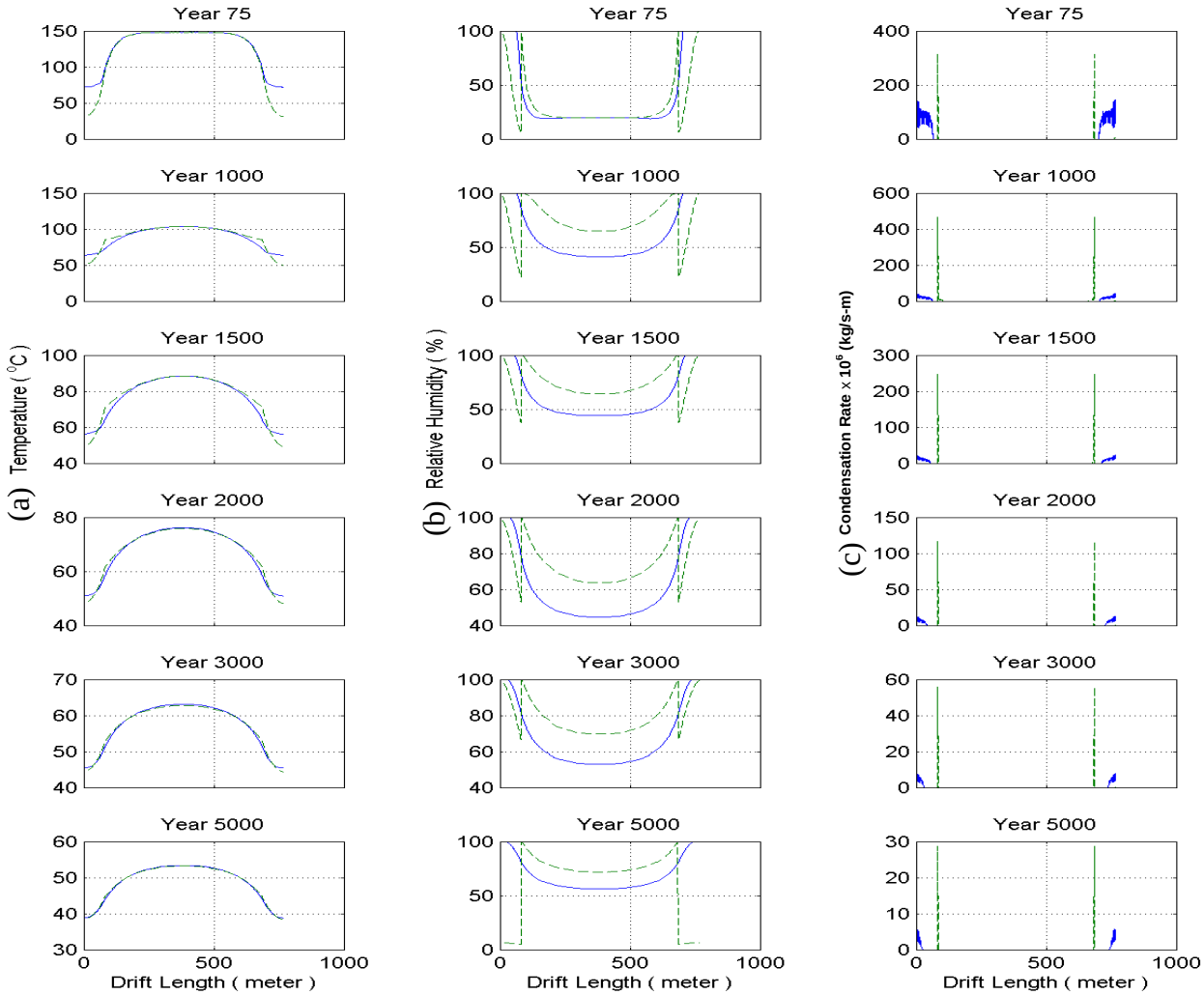

Figure 7. Axial distribution of (a) drift wall temperature, (b) relative humidity, and (c) condensation rate at selected post-closure time divisions using an axial moisture dispersion coefficient of 0.1 m^2/s (solid line for the case of unheated sections not sealed and dashed line for the case of unheated sections sealed off).

ACKNOWLEDGEMENT

The work is supported by the Director, Office of Civilian Radioactive Waste Management, Office of Science and Technology and the International, of the U.S. Department of Energy.

References

[1] Bahrami, D. and Danko, G., 2006. *Thermal-Hydrologic Model of an Alternative Waste Package Design for Yucca Mountain Repository*. Journal of Nuclear Technology, May, Vol. 154.

[2] Pruess, K., C. Oldenburg, and G. Moridis, 1999. *TOUGH2 User's Guide, Version 2.0*. Report LBNL-43134, Lawrence Berkeley National Laboratory, Earth Sciences Division, Berkeley, California.

[3] Danko, G., 2006. *Functional or Operator Representation of Numerical Heat and Mass Transport Models*, *Journal of Heat Transfer*, February 2006, Vol. 128, 162-175.

[4] Webb, S. W. and Itamura M. T., 2004. *Calculation of Post-Closure Natural Convection Heat and Mass Transfer in Yucca Mountain Drift*s. Proceedings of ASME, Heat Transfer/Fluid Engineering, July 11-15, Charlotte, NC.

[5] Bechtel SAIC Company, 2004. *In-drift natural convection and condensation*. Yucca Mountain Project Report, MDL-EBS-MD-000001 REV 00, Bechtel SAIC Company, Las Vegas, NV.

[6] Danko, G. and Bahrami, D. 2005. *Coupled Hydrothermal-Ventilation Studies for Yucca Mountain Annual Report For April 2004-March 2005.* NWRPO-2005-02. Prepared for Nye County Department of Natural Resources and Federal Facilities. Pahrump, NV.

[7] Birkholzer, J., S. Mukhopadhyay, Y.W. Tsang, 2004. Modeling Seepage into Heated Waste Emplacement Tunnels in Unsaturated Fractured Rock, Vadose Zone Journal, 3, 819-836.

[8] Danko, G., Bahrami, D., 2004. *Coupled, Multi-Scale Thermohydrologic-Ventilation Modeling with MULTIFLUX* 2004 SME Annual Meeting, February 23-25, Denver, CO.

[9] Birkholzer, J., N. Halecky, S.W. Webb, P.F. Peterson, G.S. Bodvarsson, 2006. *The Impact of Natural Convection on Near-Field TH Processes at Yucca Mountain*. Proceedings, 11th International High-Level Nuclear Waste Conference, April, Las Vegas, NV.

[10] DOE, 1999. *Design Alternative Evaluation #3: Post-Closure Ventilation.* Civilian Radioactive Waste Management System Management & Operating Contractor, BCA000000-01717-2200-00003 Rev 00.

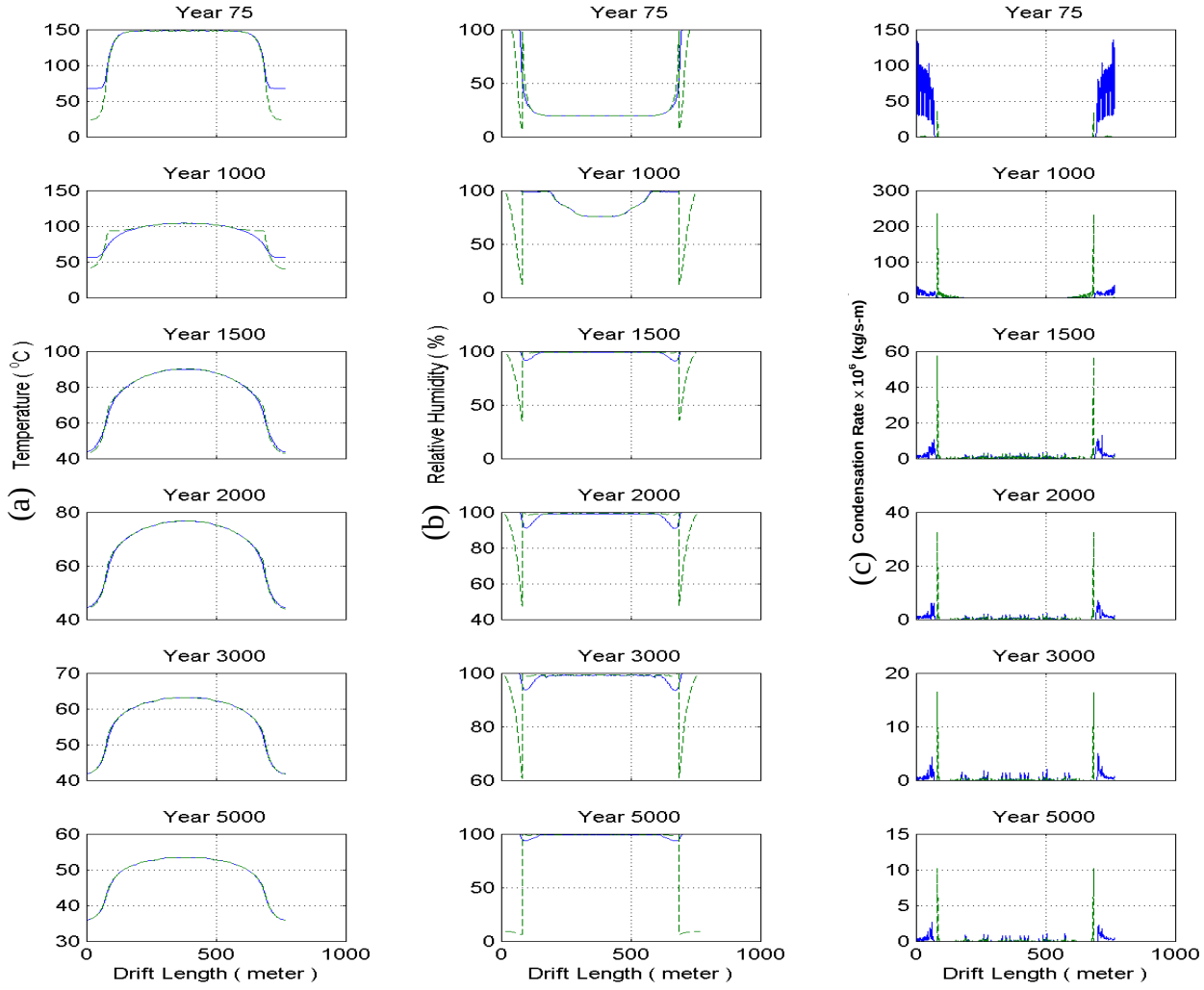

Figure 8. Axial distribution of (a) drift wall temperature, (b) relative humidity, and (c) condensation rate at selected post-closure time divisions using an axial moisture dispersion coefficient of 0.004 m^2/s (solid line for case of unheated sections not sealed, and dashed line for case of unheated sections sealed off).